Coordination Chemistry Reviews, 64 (1985) 21—39
Elsevier Science Publishers B.V., Amsterdam — Printed in The Netherlands

ELECTRONIC SPECTROSCOPY OF $M(bpy)_3^{2+}$ (M = Fe, Ru, Os), $Cr(bpy)_3^{3+}$ AND RELATED COMPOUNDS

J. FERGUSON[1], F. HERREN[2], E.R. KRAUSZ[1], M. MAEDER[1] AND J. VRBANCICH[1]
[1]Research School of Chemistry, Australian National University, G.P.O. Box 4, Canberra, A.C.T. 2601 (Australia)
[2]CIBA-GEIGY, FRIBOURG, CH-1700 (Switzerland)

ABSTRACT

Absorption and luminescence spectroscopy of the title compounds have been studied in single crystals, PVA foils and alcohol solutions. Particular attention has been given to crystal sites with defined symmetry (D_3 and C_2 for Fe, Ru, Os). The effect of 4,4' substitution in bpy has been studied for Fe, Ru, and Os complexes and significant intensity flow out of the ligand absorption bands into the metal to ligand charge transfer bands has been found for Ru and Os, consistent with back π-bonding. CD, CPL, MCD, MCPL and time resolved luminescence spectroscopy have been used to help make assignments. All of these data support a delocalized description of the luminescent states, except in fluid solutions where a viscosity dependent relaxation to a localized charge transfer state occurs. The first detailed investigation of the excited states of chromium (III) trisbipyridine in crystals is reported.

INTRODUCTION

The 2,2'-bipyridine (bpy) complexes of Ru(II) and Cr(III) have been extensively studied in relation to solar energy conversion. Both complex ions show luminescence which is relatively long lived because the radiative decays to the ground state are forbidden in the absence of spin-orbit coupling. Both complexes have three fold symmetry (D_3) and π-bonding between metal ion and ligands has strong trigonal symmetry.

The electronic states responsible for the near ultraviolet and visible spectra of $Ru(bpy)_3^{2+}$ and $Cr(bpy)_3^{3+}$ are fundamentally different. The entire visible and near ultraviolet spectrum of the former is associated with states arising from electron transfer from metal to ligand (MLCT states). The corresponding region for the latter ion contains transitions which are essentially localized on the metal ion (d-d transitions), although there is a charge transfer band in the ultraviolet region.

The ultraviolet spectra of both ions are dominated by the intense π-π^* transitions of the ligands at about 35 000 cm^{-1}. These bands are polarized primarily along the long axis of each ligand. The two center nature of the MLCT states of $Ru(bpy)_3^{2+}$ makes a detailed understanding of the absorption

0010-8545/85/$06.65

spectrum very difficult and most spectroscopic effort has gone into measurements of the luminescence from Ru and Os complexes, the Fe complex being non-luminescent. Nearly all measurements involve fluid or glassy solvent media and Crosby and co-workers (ref. 1) attempted a delineation of the number of luminescent states and their symmetry from measurements of the temperature dependences of the decay times and quantum yields. A closely spaced energy level scheme involving 3 states of symmetry A_1, E and A_2 in increasing energy order was suggested. The Crosby model is based on the assumption of thermal equilibrium among the states at all temperatures, an assumption which has recently (ref. 2) been shown to break down at temperatures below about 10 K.

The question of localization is an important one and it is strongly supported by resonance Raman scattering measurements (ref. 3). The most recent work, by Casper et al (ref.4), provides very convincing evidence that the luminescecnt states have the transferred electron localized on one ligand. These experiments do not prove that a localized description of MLCT states is the correct one, but they certainly indicate that in fluid solutions the luminescent states are localized, but this might result from some relaxation process involving an asymmetric electric field which distorts the excited states. In a delocalized model, the act of absorption or emission of light is shared by all three ligands. The theoretical treatments of Hanazaki and Nagakura (ref. 5) are localized while that given by Ceulemans and Vanquickenbourne (ref. 6) is delocalized.

We have tried to gain a better insight into the MLCT states by studies of complexes with C_2 symmetry. Here we use two types of perturbation. One is crystallographic so that the physical symmetry of the bpy ligands is distorted. The other is chemical by using mixed complexes in which one or two bpy ligands have been substituted at their 4,4' or 5,5' positions.

For our work with $Cr(bpy)_3^{3+}$ we have used single crystal spectroscopy and we have also examined chemical complexes having C_2 symmetry.

EXPERIMENTAL

Spectroscopy

A Cary model 17 spectrophotometer, a Spex 1402 double monochromator fitted with a double beam microscope attachment and Spex 1 m monochromators were used for absorption, luminescence, CD, CPL, MCD and MCPL spectroscopy. Time resolved spectra were detected with a PAR model 162 box car integrator with a Molectron DL 200 dye laser pumped by a Molectron UV 1000 nitrogen laser as excitation source.

Gas flow and liquid helium cryostats were used for temperature control and all spectroscopic measurements were made under microprocessor control. A curve analysis program was used for data manipulation and analysis.

Materials

Commercial bpy was recrystallized from hexane, 2,2'-bipyridine-4,4'-dicarboxylic acid (L) was prepared as described (ref. 7) and 2,2'-bipyridine-5,5'-dicarboxylic acid (L') was obtained from W.H.F. Sasse. The preparations of the complexes using L and L' as ligands will be given later (ref. 8). In the present work L and L' denote their diethyl esters unless otherwise stated. The structures of all complexes were confirmed by ^{1}H NMR. The analytical data are consistent with the chemical formulae.

THEORETICAL ASPECTS

Axis systems

The trigonal and cubic axis systems shown in Fig. 1 were used. The former are denoted by X,Y,Z and the latter by x,y,z. For complexes with C_2 symmetry the C_2 axis is Y.

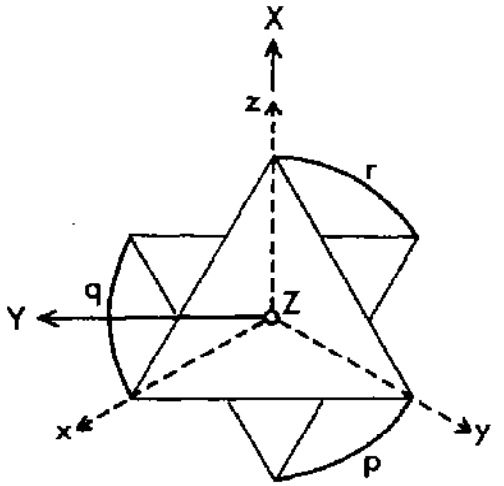

Fig. 1 Orientation of complex ion axes.

Localized model: C_2 symmetry

Consider the MLCT states arising from transfer to ligand q. For each transfer from a d orbital to q there will be one singlet and three triplet functions. The d orbitals are xy, $(xz \pm yz)/\sqrt{2}$. The 12 x 12 spin-orbit matrix can be broken into two 3 x 3, two 2 x 2 and two 1 x 1 matrices, with spin-orbit elements given in Table 1, in terms of the one electron spin-orbit coupling constant for d electrons ζ.

Matrix elements of the electric dipole operator between the ground state function and the functions S_1^q, S_2^q and S_3^q correspond to transition dipole moments along directions perpendicular to the ligand plane, parallel to the ligand long axis and parallel to the ligand short axis, respectively, if we take the π^* orbital on q to be antisymmetric with respect to C_2.

TABLE 1

Spin-orbit matrices for charge transfer between d orbitals and ligand q, C_2 localized model. Antisymmetrized singlet and triplet functions are denoted by S^q and T^q, respectively. Subscripts 1,2,3 denote transfers from xy, (xz + yz)/√2 and (xz − yz)/√2, respectively, for $M_S = 0$. The $M_S = \pm 1$ functions are denoted by subscripts 4,5 (xy → q) and 6,7,8,9 ((xz ± yz)/√2 → q). There are two equivalent sets of functions S_n^p, S_n^r etc., corresponding to equivalent transfers to ligands p and r, respectively.

	S_1^q	T_9^q
S_1^q	0	$-\zeta/\sqrt{2}$
T_9^q	$-\zeta/\sqrt{2}$	$-\zeta/2$

	T_1^q	T_8^q
T_1^q	0	$\zeta/\sqrt{2}$
T_8^q	$\zeta/2$	$-\zeta/2$

	S_2^q	T_3^q	T_4^q
S_2^q	0	$\zeta/2$	$\zeta/2$
T_3^q	$\zeta/2$	0	$-\zeta/2$
T_4^q	$\zeta/2$	$-\zeta/2$	0

	S_3^q	T_2^q	T_5^q
S_3^q	0	$-\zeta/2$	$-\zeta/2$
T_2^q	$-\zeta/2$	0	$-\zeta/2$
T_3^q	$-\zeta/2$	$-\zeta/2$	0

T_6^q, T_7^q: $\zeta/2$

Localized model: D_3

The D_3 localized functions can be obtained by operating on the C_2 functions with C_3. In complex form they are:

$$S_{\pm}^1 = \mp(S_1^q + \omega^{\mp} S_1^p + \omega^{\pm} S_1^r)/\sqrt{3}; \quad A^1 = (S_1^q + S_1^p + S_1^r)/\sqrt{3} \qquad (1)$$

$$S_{\pm}^2 = \mp(S_2^q + \omega^{\mp} S_2^p + \omega^{\pm} S_2^r)/\sqrt{3}; \quad A^2 = (S_2^q + S_2^p + S_2^r)/\sqrt{3} \qquad (2)$$

$$S_{\pm}^3 = \mp(S_3^q + \omega^{\mp} S_3^p + \omega^{\pm} S_3^r)/\sqrt{3}; \quad A^3 = (S_3^q + S_3^p + S_3^r)/\sqrt{3} \qquad (3)$$

where $\omega^{\pm} = \exp(\pm 2\pi i/3)$

The corresponding real D_3 localized functions can easily be obtained, e.g., $S_X^1 = (S_+^1 - S_-^1)/\sqrt{2}$; $S_Y^1 = -i(S_+^1 + S_-^1)/\sqrt{2}$ for q antisymmetric about C_2. These

functions are equivalent to those of Hanazaki and Nagakura (ref. 5). The localized D_3 model predicts metal to ligand transfer term intensity in the transition to only one E state.

Delocalized model

Delocalized descriptions have been given for singlet states (ref. 6) as well as singlets and triplets (ref. 9,10). It can be easily shown that the three delocalized E functions correspond to symmetry determined combinations of the D_3 localized basis functions. The relationships are:

$$1E_{\pm} = -(S^1_{\mp} + \sqrt{2}S^2_{\mp})/\sqrt{3} \quad (4)$$

$$2E_{\pm} = (S^1_{\pm} - (1/\sqrt{2})S^2_{\pm} \pm \sqrt{(3/2)}iS^3_{\pm})/\sqrt{3} \quad (5)$$

$$3E_{\pm} = \mp(S^1_{\mp} - (1/\sqrt{2})S^2_{\mp} \pm \sqrt{(3/2)}iS^3_{\mp})/\sqrt{3} \quad (6)$$

We note that transitions to 2E and 3E carry equal transfer term intensity while that to 1E has zero intensity, for π^* antisymmetric. If π^* is symmetric then the transfer term intensity is given by the S^2 functions and all three E states will have absorption intensity in the ratio 1E:2E:3E::4:1:1, in agreement with the predictions of Ceulemans and Vanquickenbourne (ref. 6).

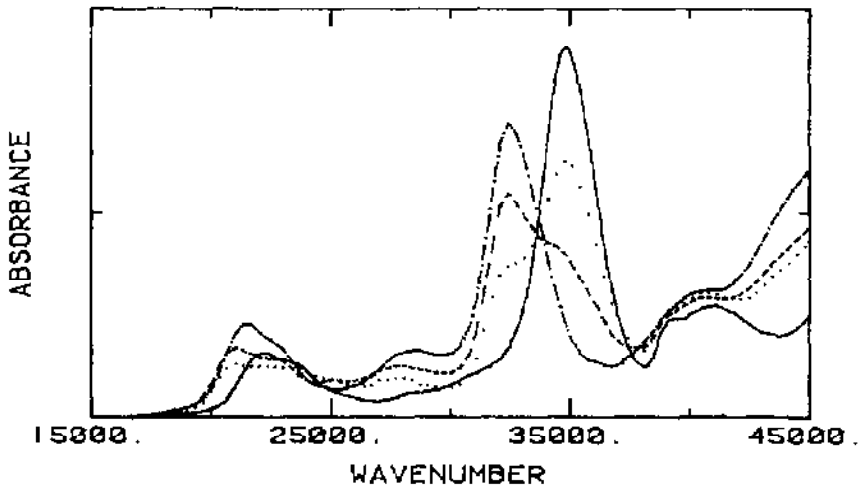

Fig. 2. Absorption spectra of $Ru(bpy)_3^{2+}$ (——), $Ru(bpy)_2L^{2+}$ (....), $RubpyL_2^{2+}$ (----) and RuL_3^{2+} (-·-·) in ethanol at room temperature, plotted so that their integrated absorption intensities are normalized.

RESULTS AND DISCUSSION: $M(BPY)_3^{2+}$

Overall spectral features

It is common practice to consider the lowest energy MLCT band in isolation. However, simple data analysis shows that the visible and ultraviolet spectra must be considered as a whole. Examination of the effect of pH on the absorption spectrum of $Ru(bpy)_2L^{2+}$ (acid or base forms of L) in water (ref. 11) provides the result that although the absorption spectrum with the acid (pH = 0.40) and base (pH = 4.1) forms of L in the complex appear to be substantially different, the integrated absorption intensities of the complex with L in its

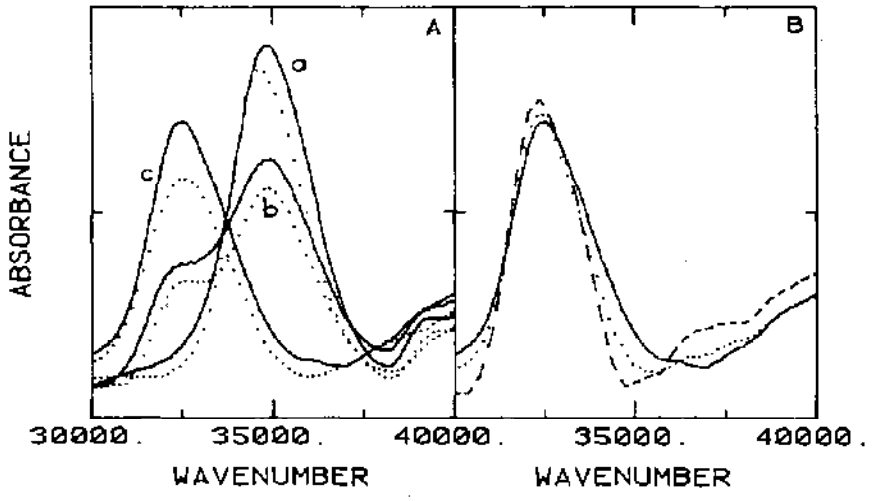

Fig. 3. (A) Ligand absorption bands of $M(bpy)_3^{2+}$ (a), $M(bpy)_2L^{2+}$ (b) and ML_3^{2+} (c) (Ru, full lines; Os, broken lines). The Os spectra have been displaced to higher wavenumber by 350 cm^{-1}. (B) Ligand absorption spectrum of RuL_3^{2+} (——) and synthesized spectra (...., ----, see text).

acid and base forms are identical for the spectral region 18 000 - 38 000 cm^{-1}, which includes all MLCT bands and the main π-π^* ligand band. Absorption intensity can therefore move between ligand bands and MLCT bands, dependent on what appear to be rather subtle changes in the ligands. We apply this observation to the absorption spectra of $Ru(bpy)_3^{2}$, $Ru(bpy)_2L^{2+}$, $RubpyL_2^{2+}$ and RuL_3^{2+}, measured in ethanol, plotted so that their integrated absorption intensities are normalized for the visible and ultraviolet regions which include the main ligand band (Fig. 2). These spectra reveal an approximate isosbestic point near 33 000 cm^{-1}. Analogous results were obtained for the corresponding Os complexes (ref. 8). and the presence of the isosbestic points supports the conclusion that the intensity can flow from ligand into the MLCT bands, providing new insight into the relationship between these two types of band systems. We defer discussion of the MLCT bands (ref. 8) and consider the ligand bands. We show in Fig. 3A the ligand absorption bands of $M(bpy)_3^{2+}$,

$M(bpy)_2L^{2+}$ and ML_3^{2+} (M = Ru, Os) in which the osmium spectra have been displaced by 350 cm^{-1} to bring the two sets of approximate isobestic points into closer alignment.

An important observation to be made from Fig. 3A is that the ligand bands are, to a very good approximation, additive so far as their intensities, shapes and positions are concerned. It follows therefore, that inter-ligand coupling is not important for spectral analysis of the ligand bands. The large 'exciton' or excitation resonance coupling energies proposed by Mason and co-workers (ref. 12) are grossly overestimated. They must be much smaller than the spectral band widths, which supports the conclusions reached earlier by Bray et al (ref. 13). Interpretation of the CD must be made within a vibronic coupling model and the point dipole-dipole approximation for interaction energies is quantitatively very poor. We can illustrate this conclusion further by carrying out a 'synthesis' of the absorption band of RuL_3^{2+} from those of $Ru(bpy)_2L^{2+}$ (....) and $RubpyL_2^{2+}$ (----), by subtraction of the Rubpy absorption taken as appropriate fractions of the $Ru(bpy)_3^{2+}$ spectrum. The result is given in Fig. 3B and the very close agreement between these two synthesized spectra and the actual spectrum is an indication of the correctness of the conclusion. We notice from Fig. 3A that the intensity of the L band is less than that of the bpy band in each case, while for the same complex ion configuration, both ligand intensities are less for Os than Ru. In each case the missing intensity is found in the MLCT bands. Further analysis of the ligand band absorption will be given elsewhere (ref.8).

If we assume that the visible MLCT band corresponds to transfer into the lowest π^* orbital (6' in Gondo's notation (ref.14)), then there should be another pair of MLCT states about 5 000 cm^{-1} higher in energy (transfer to orbitals 4' and 5'). A fourth state should lie about 12 000 cm^{-1} above the lowest MLCT state, if we neglect configuration interaction. The absorption spectra show two regions of MLCT band lying below the ligand bands. We rather arbitrarily break up these regions into MLCT1 (corresponding to the region 18 000 - 27 500 cm^{-1} of the $Ru(bpy)_3^{2+}$ spectrum), MLCT2 (27 500 - 32 000 cm^{-1}) and the ligand band (32 000 - 38 000 cm^{-1}). This procedure is less satisfatory for the Os complex because of the overlap between the triplet bands of the MLCT2 bands and the singlet bands of MLCT1. The relative intensities are given in Table 2.

We see that 4,4' substitution increases substantially the absorption intensities of the MLCT bands of Ru and Os complexes but not those of the Fe complex.

Circular dichroism

The CD of the tris bpy complexes has been extensively studied (ref. 12) and there have been a number of attempts to interpret the CD of the MLCT bands. It has generally been assumed that the CD of the ligand bands has its origin in the dipole coupling of transition moments in each ligand (polarized along the long ligand axis). The CD of the MLCT region has been ascribed to either

TABLE 2
Relative intensities of the MLCT1, MLCT2 and ligand bands in the complexes $M(bpy)_3^{2+}$ and ML_3^{2+}, M = Fe, Ru and Os

Metal	Ligand	MLCT1	MLCT2	$\pi-\pi^*$
Fe	bpy	12%	10%	78%
Fe	L	12	10	78
Ru	bpy	16	12	72
Ru	L	21	20	59
Os	bpy	19	19	62
Os	L	32	17	51

direct borrowing of rotational strength from the ligands or by coupling between

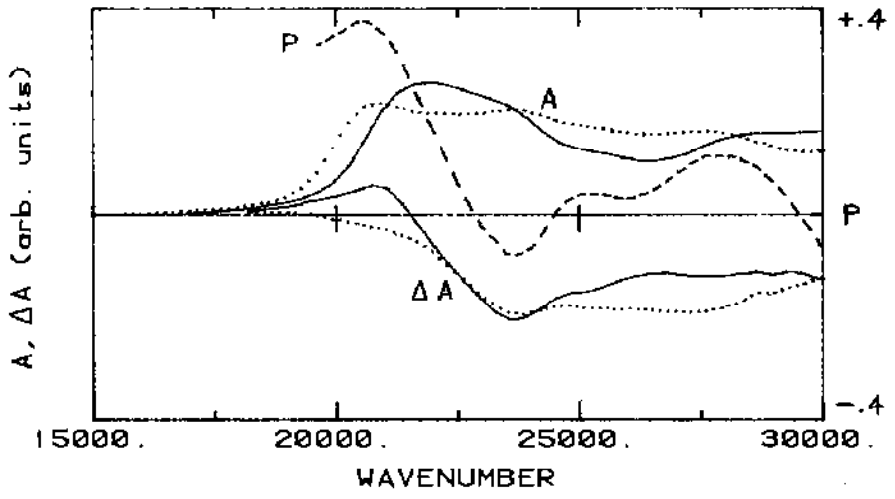

Fig. 4. CD (ΔA), absorbance (A) and luminescence polarization ratio (P) of $Ru(bpy)_2L^{2+}$ for L in its acid (....) and base (----) forms (ΔA and A) and diethyl ester form (P).

the MLCT transition moments and induced ligand moments (ref.15). An example suffices to show that neither mechanism accounts for the observed CD.

Fig. 4 shows the CD of $Ru(bpy)_3^{2+}$, where L is the acid or base form of L, measured at two values of pH corresponding to the full acid and base forms of L. Fig. 4 also contains the absorption spectra of acid and base forms as well as the luminescence polarization ratio (P) of the diethyl ester form of L (see ref.11). For pH = 4.1 L has the base form and the CD (and spectral band shape) is similar to that of $Ru(bpy)_3^{2+}$. Replacement of the two protons (pH = 0.40) removes the low energy CD completely (similar results were obtained for the corresponding Os complex ion). The lowest energy band which develops on protonation corresponds to charge transfer to ligand L (orbital jump $(xz - yz)/\sqrt{2} \rightarrow q$), shown by the high positive value of P. If coupling were important this band should also show CD. Similarly, although this band is predominently polarized M to L, there should be a much weaker band close by, corresponding to an orbital jump $(xz + yz)/\sqrt{2} \rightarrow q$, with intensity stolen from the L ligand band. If stolen CD were important then it should have the same sign as the ligand CD, which is positive for both acid and base forms of L (Fig. 5). We note that the CD and P values are both consistent with a bpy energy level order B > A. Also, protonation of L lowers its excited state relative to the bpy states and reduces the interaction between it and the B component of the bpy pair of states, thereby making the B and A bpy states closer in energy and the overall CD is reduced by this cancellation. The CD from the B state of L appears to be relatively strong only because of the near cancellation of the contributions from the bpy B and A states.

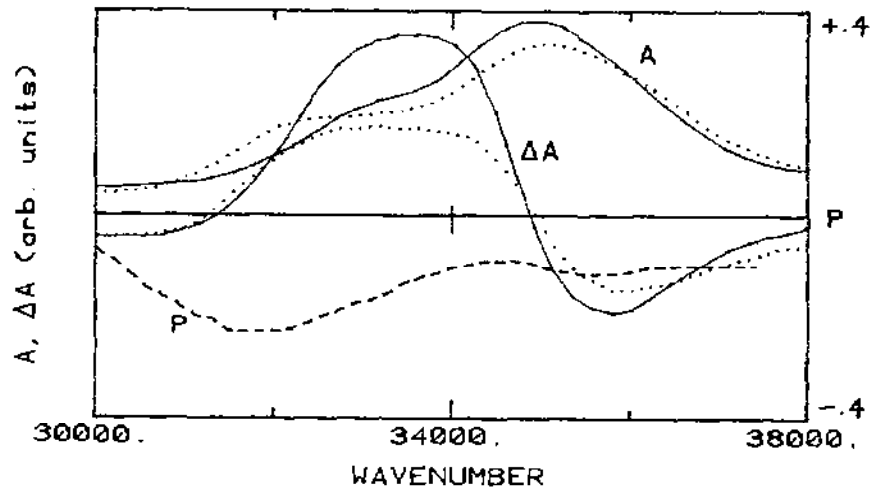

Fig. 5 Same as for Fig. 4 but in the ligand region.

The interpretation of the MLCT CD was resolved by single crystal measurements (ref. 16). The metal centered magnetic moments are intrinsic and have their origins in covalency between metal ion and ligand. The crystal CD records only contributions from E states while the solution CD is composed of both E and A_2 contributions. The CD of the Os complex is of particular importance and it is included in Figs. 6 and 7.

Magnetic circular dichroism

The first attempts to measure MCD of charge transfer complexes of Ru^{2+} were made by Hollebone et al (ref.17) for $Ru(phen)_3^{2+}$. They concluded that B terms dominate the MCD in the visible MLCT region. Our measurements using single crystals and PVA foils at liquid helium temperatures are dominated by A terms. We concentrate on the MCD of $Os(bpy)_3^{2+}$ and Fig. 6 shows the MCD and CD of a resolved sample in PVA at 5.5 K together with its absorption spectrum.

We note that the overall MCD is significantly weaker than the natural CD and in the ligand region the MCD is essentially non-existent. The absence of a magnetic moment in the ligand excited state is consistent with the lack of significant inter-ligand interaction observed in the absorption spectra. The strongest features are at 15 000 cm^{-1} and 20 400 cm^{-1} which are A terms of opposite sign. These conclusions are reinforced from the CD and MCD of the

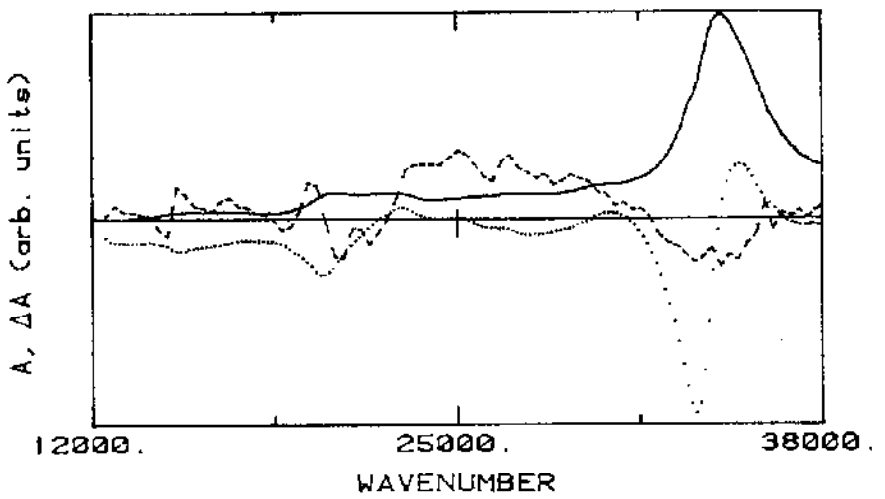

Fig. 6 Absorption spectrum (——), CD (....) and MCD (----, x5) of $Os(bpy)_3^{2+}$ in PVA at 5.5 K.

same ion in $Zn(bpy)_3(BF_4)_2$. The same A terms are more clearly evident and there is another A term centered at 22 700 cm^{-1}. Considering the lowest energy A term (Fig. 7A) and making the assumption that the excited state g ~ 1 we can

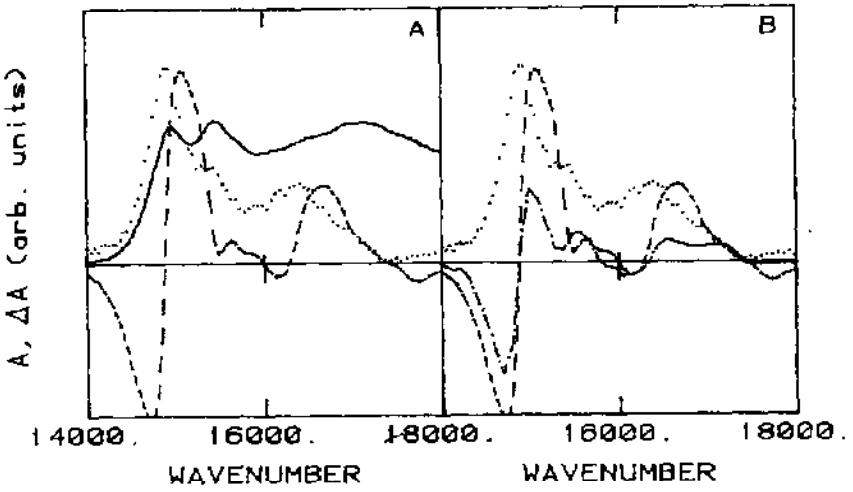

Fig. 7. A: Same as for Fig. 6 but in $Zn(bpy)_3(BF_4)_2$. B: CD (....), MCD (----) and simulated MCD (-·-·-).

use the observed CD band shape to simulate the observed A term. We simply displace the spectrum by an amount equal to the Zeeman splitting and subtract

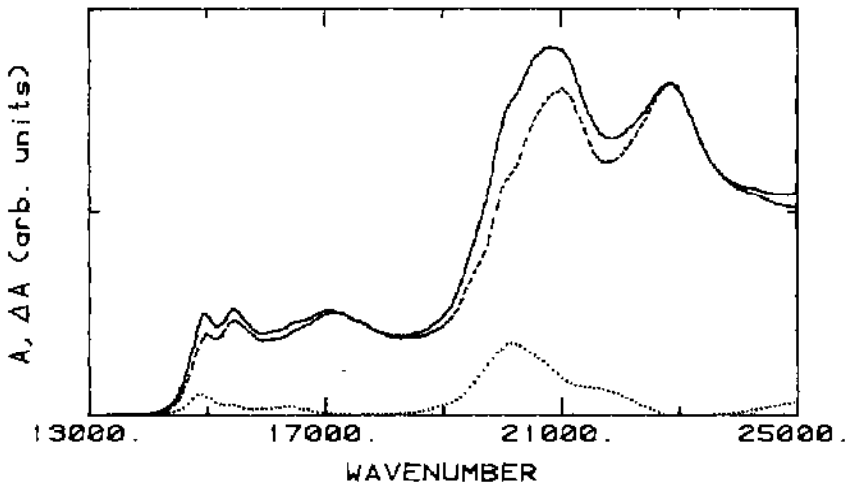

Fig. 8. Absorption spectrum of Os in $Zn(bpy)_3(BF_4)_2$ (——), absorption spectrum of bands which carry CD (....), absorption spectrum of bands with no CD (----).

the undisplaced spectrum from it. This process provides a simulation of the observed A term and from the magnitude of the latter we can estimate the absorbance of the band which carries the CD, shown in Fig. 8. Subtraction of this calculated spectrum from the observed absorption spectrum provides the absorption spectrum of the bands which carry neither CD no MCD. We see that the resultant spectrum has lost much of the pronounced shoulder on the low energy side of the most intense spin-allowed band, which characterizes the observed spectrum, so that the remaining two spin-allowed bands have equal intensities. It is perhaps fortuitous that agreement between experiment and theory for the delocalized model is now good because the same theory predicts no transfer term intensity for the transition $^1A_1 \rightarrow {}^1E$ which is the band which has been subtracted.

The result for the triplet region is the more significant as it shows that the two lowest energy bands (assigned to excited states 4E and 5E ref. 10) have neither CD nor MCD. Both are associated with a weak band nearly degenerate with the lowest energy band. We assign it to the transition to 11E' which mixes via spin-orbit coupling with 1E. The theory then accounts for the observed CD in one spin-allowed band and only one triplet band. The observed intensity ratio of spin-allowed to spin-forbidden intensities (84:16) is in very good agreement with the predicted ratio (82:18).

Although the theory appears to account for the CD sucessfully the same cannot be said of the MCD. Here, the very reasonable assumption that the magnetic moments are determined by the metal ion means that the g factor for 1E should be zero and non-zero for 2E and 3E. In addition 4E and 5E should have non-zero g fators and yet we do not observe MCD for either. The whole problem of the MCD is a puzzle at present and requires further investigation. We note finally, that the MCD of the Ru complexes $Ru(bpy)_3^{2+}$, RuL_3^{2+} and $RuL'_3{}^{2+}$ show features analogous to those in Figs. 6 and 7, so there must be a common interpretation for all the MCD data.

CPL and MCPL

The observation of CPL and MCPL for Ru in $Zn(bpy)_3(BF_4)_2$ has been reported earlier (ref. 2) and we have extended these measurements to Os in the same host. As they will be given in detail later (ref. 18) we summarize the relevant results here.

At very low temperatures (1.5 K) we find CPL and MCPL with the same band shape and position. However, their spectral distributions do not coincide with the steady state luminescence which is broader and displaced to lower energy. Increase of temperature (to 90 K) leads to an increase of band width of both CPL and MCPL, but no change of position, while the steady state luminescence

shifts to higher energy, its band shape narrows and it becomes the same as those of the CPL and MCPL.

The sign of the MCPL is opposite to that which would be observed from the state which gives the A term in the MCD and its C term behaviour is consistent with an E state. Considerations of band shape and band position are consistent with CPL and MCPL both arising from the same E state. The only discrepancy is the temperature dependence of the CPL. Cooling from 90 K leads to a reduction of the amplitude of the CPL signal to zero at about 15 K and below this temperature the CPL signal appears with opposite sign. Presumably this behaviour indicates a change in the electric dipole mechanism which alters the phase of the transition moments and as it only occurs in the excited state it must be related to some temperature dependent relaxation phenomenon. At present we have no explanation for this result.

Triplet absorption spectra

Triplet absorption spectra are most clearly seen in the spectrum of $Os(bpy)_3^{2+}$ because of the large spin-orbit coupling. Measurements taken with Os in D_3 sites (in $Zn(bpy)_3(BF_4)_2$ (Fig. 7) or in $Ru(bpy)_3(PF_6)_2$) show two bands separated by about 500 cm^{-1}. The effect of a crystallographic distortion of C_2 symmetry reveals the polarization properties of these two states and also the presence of a third much weaker band corresponding to the state which carries the CD and MCD shown in Figs. 6 and 7. Fig. 9 shows the polarized absorption of Os in $Zn(bpy)_3(PF_6)_2$ and the three lowest triplet states are shown by labels a,b and c. These three states appear (split) in both crystal polarizations and are derived from states of E representation in the D_3 group. Another state having σ polarization in the crystal, corresponding to an A_2 triplet state, observable in the host $Ru(bpy)_3(PF_6)_2$, should appear in the same region and is probably the shoulder at 15 250 cm^{-1} denoted by d in Fig. 9. Because of the orientation of the complex ion in the host $Zn(bpy)_3(PF_6)_2$ transitions to A_2 states will appear only in σ polarization and band d is absent in π polarization. The weak band correponding to band labelled b must be the componenta of the E state which is responsible for the CD of Os in a D_3 site (Figs. 6 and 7). Its close proximity to the more intense lowest energy band is consistent with this conclusion and it is therefore assigned to $^1E'$ which mixes via spin-orbit coupling with ^1E (ref. 10). Its polarization is consistent with this assignment.

Luminescence spectra

Fig. 9 contains examples of the luminescence from Os in a C_2 site and the striking feature of the spectra is the gap (Stokes shift) between absorption

and luminescence bands which develops on cooling (ref.10). This indicates excited state relaxation. The Stokes shift is not so obvious from measurements made in glassy solvents because of the greater band widths. Further cooling to 2 K leads to a slight increase in the band gap. Similar experiments with Ru show an analogous Stokes shift down to about 8 K. Below this temperature there is a reduction in the band gap because of the appearance of a weak broad shoulder on the high energy edge of the luminescence band. At the same time

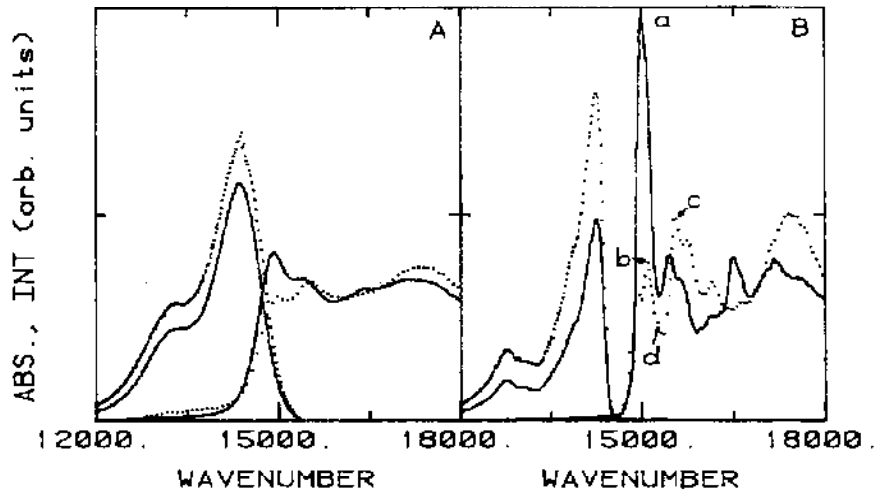

Fig. 9. Absorption and luminescence polarized spectra (π, —— ; 2σ, ...) of Os in $Zn(bpy)_3(PF_6)_2$ at room temperature (A) and 7 K (B).

the body of the luminescence intensity shifts to lower energy. Subtraction of the higher temperature contribution from a 2 K spectrum reveals the luminescence spectrum which appears below about 8 K and dominates the overall emission at 2 K (Fig. 10).

The weak origin and more intense vibronic side-band indicate two different mechanisms for radiative emission. The zero phonon band appears because of the C_2 perturbation which mixes the triplet state with another triplet state having some singlet character via spin-orbit coupling. The more intense vibrationally induced band occurs by vibrational mixing with another triplet state which has different singlet character and opposite polarization to that involved in the zero phonon band. This spectrum dominates the 2 K emission and was first reported by Crosby (ref.19) who assigned it to a forbidden transition from an A_1 state in D_3. In our analysis its linear polarization (ref. 2) is consistent with an E assignment and its behaviour with a pure triplet (primarily 6E (ref.10) whose C_2 localized analogoues are T_1^q and T_8^q, Table 1). Its

forbiddeness is also revealed by the time resolved spectroscopy which shows that the spectra with longest delays have a red-shifted intensity distribution approaching that in Fig. 10.

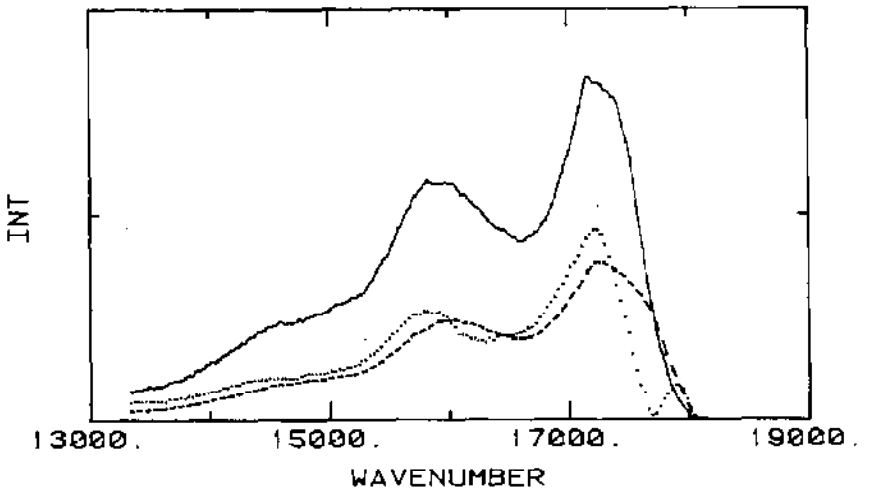

Fig. 10. Luminescence spectra of Ru in $Zn(bpy)_3(PF_6)_2$ (π, —— and σ,----) and the σ spectrum (....) which appears below about 8 K (all at 2 K).

The properties of the luminescent state of both Ru and Os are consistent with assignments to E states for the emission at relatively low temperatures, one of which is a pure triplet in D_3 symmetry. Two other states dominate the luminescence, except for Ru below about 8 K, and their likely assignments are 4E and 11E' which gain intensity via spin-orbit coupling from singlet state 2E and 1E respectively.

Van Houten and Watts (ref. 20) reported the temperature dependence of the luminescence spectrum of $Ru(bpy)_3^{2+}$ in ethylene glycol. Contrary to our results in crystals they found a blue shift on cooling, between 273 and 196 K, and a marked change of band shape. Significantly, the emission spectrum in PVA foils does not show the same phenomena on cooling and it is possible that the the ethylene glycol result is connected with an increase of solvent viscosity which inhibits an environmental relaxation responsible for charge localization in fluid solutions. If this were so then the room temperature spectrum would correspond to emission from a localized species, presumably with C_2 symmetry. This interpretation can be tested by using another less visoous solvent medium and we used an ethanol/methanol mixture. We found that between room temperature and 180 K there is little significant change of emission band shape. Below this temperature however, on the formation of a glass, the

emission shifts to the blue and develops structure (Fig. 11). We conclude therefore, that the room temperature emission spectrum in fluid solutions is associated with a localized charge transfer state as required by the resonance Raman scattering experiments.

Time resolved luminescence

The non-thermalization of $Ru(bpy)_3^{2+}$ luminescence in crystals and PVA has been reported earlier (ref. 2). This work has been extended to other Ru complexes containing L and L' ligands with C_2 and D_3 symmetry. All show analogous behaviour at 2 K, i.e., the development of a long lived component with an intensity distribution displaced from that of the shorter time component. As either D_3 or C_2 complexes will have states which are pure triplets we assign the long lived components to such states which can emit when non-thermalization of the excited states occurs at very low temperatures.

Time resolved luminescence spectra of $Ru(bpy)_3^{2+}$ in glassy solutions, close to the glass transition, show the time dependent spectral shift from delocalized to localized charge transfer luminescent states expected from the spectra in Fig. 11 (ref. 21).

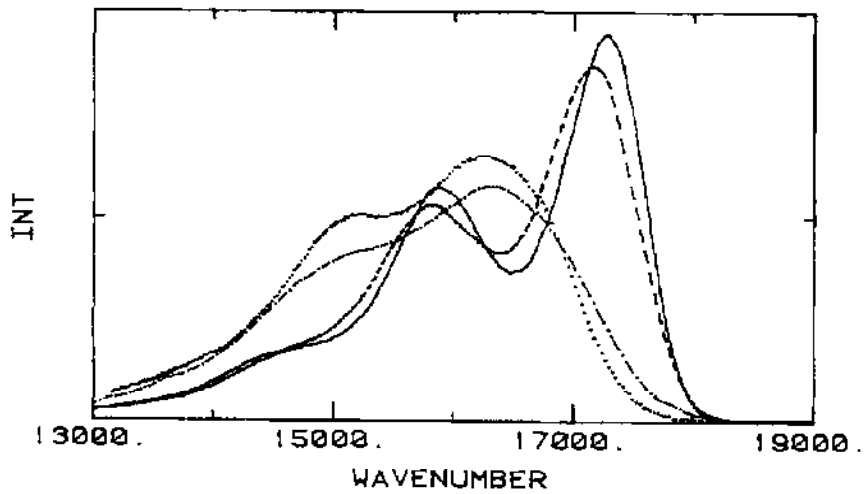

Fig. 11. Luminescence spectra of $Ru(bpy)_3^{2+}$ observed at various temperatures in ethanol:methanol 4:1, -·-·-, 225 K;·····, 180 K, ----, 125 K, ——, 95 K.

Charge localization

Our measurements of CD, CPL, MCD and MCPL as well as linear polarization of absorption and emission in $Zn(bpy)_3(PF_6)_2$ are all consistent with behaviour expected from a delocalized description of the excited states. The most important argument for delocalization of the luminescent states stems from the

MCPL C term behaviour characteristic of E states. The likely explanation for the resonance Raman experiments has been suggested and involves charge localization which occurs in fluid solutions because of environmental relaxation.

RESULTS AND DISCUSSION: $Cr(bpy)_3^{3+}$

Koenig and Herzog (ref. 22) have made an assignment of the aqueous solution absorption spectrum of $Cr(bpy)_3^{3+}$ on the basis of crystal field theory. All of the bands, with the exception of those due to the ligand at 33 000 and 42 000 cm^{-1}, were assigned to d-d transitions. Our measurements, based on single crystal absorption spectra, do not support d-d assignments for all of the spin-allowed bands. However, as solar energy applications are concerned with the lowest excited states, we defer consideration of the quartet states (ref. 23) and deal only with transitions to the doublet states which are d-d in nature. The two lowest energy absorption bands, at 13 750 and 14 500 cm^{-1}, were assigned by Koenig and Herzog as transitions to ^2E and $^2T_1$, respectively, and our analysis supports these assignments.

The intensity of the transition to ^2E is comparable to those in other trigonal Cr^{3+} ions. Absorption spectra of $Cr(bpy)_3(PF_6)_3$ single crystals reveal the two components of the ^2E state, split by the combined action of the trigonal field and spin-orbit coupling. The site symmetry of the Cr is D_3 (ref. 23) so we use the theoretical model developed by Sugano and Tanabe (ref. 24) for the analysis of the absorption spectrum. The spectra (Fig. 12) show

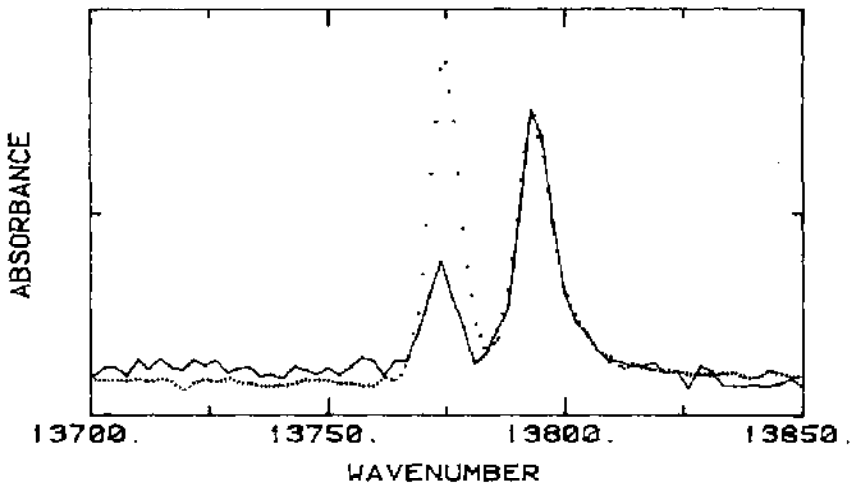

Fig. 12. Polarized (σ.....: π, ——) absorption spectra of $Cr(bpy)_3(PF_6)_3$ at 7 K. σ and π refer to electric vector directions perpendicular and parallel, respectively, to the crystal C_3 axis.

that the higher energy lines appear equally intense for σ and π polarizations, while the lower energy line is approximately three times stronger for σ polarization. The splitting is 19 ± 1 cm^{-1}, somwewhat less than for the R lines in ruby. We can use this splitting to obtain an estimate of the trigonal field splitting parameter and its sign once we have assigned each component. This is straightforward as the theory predicts that the transition to $2\bar{A}$ should have $\sigma > \pi$, while that to $\bar{E}$ should have $\sigma : \pi = 5:1$. We therefore assign the higher energy component to $2\bar{A}$.

The splitting of ^2E ($W(2\bar{A}) - W(\bar{E})$) is equal to $4K\zeta/(W(^2E) - W(^2T_2))$, where K is the trigonal field splitting parameter, ζ is the spin-orbit coupling constant and the denominator is the energy difference between ^2E and $^2T_2$ states. If we assume that $\zeta = 220$ cm^{-1} then we obtain $K = -140$ cm^{-1} from the observed splitting and the energies of ^2E and $^2T_2$ (13 800 and 20 100 cm^{-1}, respectively). The negative sign indicates that the e component of the trigonal t_2 orbitals lies lower in energy than the a_1 component.

We can then use the theory of Sugano and Tanabe (ref. 24) to calculate the splittings of the $^2T_1$ and $^2T_2$ states. The theory also predicts the polarizations of the components which can be compared with experiment. For the present purpose we conclude that the luminescent states of $Cr(bpy)_3^{3+}$ correspond to the ^2E and $^2T_1$ electronic states of Cr^{3+} in a relatively small trigonal field and these states are very well described by crystal field theory.

Acknowledgment. M.M. gratefully acknowledges the support of the Swiss National Science Foundation through the award of a Postdoctoral Fellowship.

REFERENCES

1 a. G.D. Hager and G.A. Crosby, J. Am. Chem. Soc., 97 (1975) 7031-7037.
b. G.D. Hager and G.A. Crosby, J. Am. Chem. Soc., 97 (1975) 7037-7042.
c. K.W. Hipps and G.A. Crosby, J. Am. Chem. Soc., 97 (1975) 7042-7048.
2 J. Ferguson and E.R. Krausz, Chem. Phys. Letters, 93 (1982) 21-25.
3 a. R.F. Dallinger and W.H. Woodruff, J. Am. Chem. Soc., 101 (1979) 4391-4393.
b. P.G. Bradley, N. Kress, B.A. Hornberger, R.F. Dallinger and W.H. Woodruff, J. Am. Chem. Soc., 103 (1981) 7441-7446.
4 J.V. Casper, T.D. Westmoreland, G.H. Allen, P.G. Bradley, T.J. Meyer and W.H. Woodruff, J. Am. Chem. Soc., 106 (1984) 3492-3500.
5 I. Hanazaki and S. Nagakura, Inorg. Chem., 8 (1969) 648-654.
6 A. Ceulemans and L.G. Vanquickenbourne, J. Am. Chem. Soc., 103 (1981) 2238-2241.
7 G. Sprintschnich, H.W. Sprintschnick, P.I. Kirsch and D.G. Whitten, J. Am. Chem. Soc., 99 (1977) 4947-4954.
8 J. Ferguson and F. Herren, to be published.
9 E.M. Kober and T.J. Meyer, Inorg. Chem., 21 (1982) 3967-3977.
10 J. Ferguson and F. Herren, Chem. Phys., 76 (1983) 45-59.
11 J. Ferguson, A.W-H. Mau, Chem. Phys., 68 (1979) 21-24.
12 a. S.F. Mason, Inorganica chim. Acta Reviews, 2 (1968) 89-109.
b. S.F. Mason, B.J. Peart and R.E. Waddell, J Chem. Soc. Dalton

(1973) 944-949.
13 R.G. Bray, J. Ferguson and C.J. Hawkins, Aust. J. Chem., 22 (1969) 2091-2103.
14 Y. Gondo, J. Chem. Phys., 41 (1964) 3928-3938.
15 R.D. Peacock and B. Stewart, Coord. Chem. Rev., 46 (1982) 129-157.
16 J. Ferguson, F. Herren and G.M. McLaughlin, Chem. Phys. Letters, 89 (1982) 376-380.
17 B.R. Hollebone, S.F. Mason and A.J. Thomson, Symp. Faraday Soc., 3 (1969) 146-152.
18 J. Ferguson, E.R. Krausz and J. Vrbancich, to be published.
19 D.C. Baker and G.A. Crosby, Chem. Phys., 4 (1974) 428-433.
20 J. van Houten and R.J. Watts, J. Am. Chem. Soc., 98 (1976) 4853-4858.
21 J. Ferguson, E.R. Krausz and M.Maeder, to be published.
22 E. Koenig and S. Herzog, J. Inorg. Nucl. Chem., 32 (1970) 585-599.
23 J. Ferguson and M. Maeder, to be published.
24 S. Sugano and Y. Tanabe, J. Phys. Soc. Japan, 13 (1958) 880-899.